

## Structural effects of pressure on monoclinic chlorite: A single-crystal study

P.F. ZANAZZI,\* M. MONTAGNOLI, S. NAZZARENI, AND P. COMODI

Dipartimento di Scienze della Terra, Università di Perugia, Piazza Università, I-06100 Perugia, Italy

### ABSTRACT

A single-crystal X-ray diffraction study in a diamond anvil cell up to 5.41 GPa was carried out on a clinochlore [monoclinic polytype *I1b-2*, S.G. *C2/m*,  $(\text{Mg}_{9.09}\text{Fe}_{1.01}^{2+}\text{Mn}_{0.02}\text{Ti}_{0.01}\text{Cr}_{0.02}\text{Al}_{1.80})_{\Sigma=11.95}(\text{Si}_{6.35}\text{Al}_{1.65})_{\Sigma=8}\text{O}_{20}(\text{OH})_{16}$ ] from Val Malenco, Italy.

The bulk modulus of monoclinic clinochlore calculated by fitting unit-cell volumes and pressures to a third-order Birch-Murnaghan Equation of State (EoS), is  $K_0 = 71(9)$  GPa with  $K' = 8(5)$ . Axial compressibility values were  $\beta_{0a}^{\text{EoS}} = 3.8(1)$ ,  $\beta_{0b}^{\text{EoS}} = 3.6(1)$ , and  $\beta_{0c}^{\text{EoS}} = 5.4(5) \cdot 10^{-3}$  GPa<sup>-1</sup>, showing that axial anisotropy is much less than that found for other phyllosilicates. Compressibility data are in fair agreement with literature data, which are based on powder neutron and synchrotron diffraction methods. Results were compared with the behavior of the triclinic polytype of similar composition and coexisting in the same rock. Symmetry has little overall influence on compressibility, but compared with the triclinic polytype of similar composition and coexisting in the same hand specimen, the monoclinic polytype is slightly less rigid.

Comparison of structural refinements at different pressures showed that structural deformations mainly affect the interlayer region, where hydrogen bonds are important for the structural properties of the phase. The mean decrease in OH-O distances was about 9% in the pressure range 0–5 GPa. Structural behavior was very similar to that found for the triclinic polytype.

Although energy differences between polytypes are relatively small, their compressional behavior may have implications in terms of relative stability. A computation of molar volume applying an isothermal EoS shows that the triclinic polytype is lower in volume up to 0.9 GPa, above which the volume of the monoclinic phase is smaller. This fact gives information on the relative stability of the two polytypes and a possible explanation for the greater abundance of the triclinic polytype in low to medium-*P* environments, as is commonly observed in nature.

**Keywords:** Chlorite, high pressure, polytypism, equation of state

### INTRODUCTION

Chlorite is a widespread family of di- and trioctahedral layer silicates. The structure of trioctahedral chlorite consists of talc-type, negatively charged T-O-T 2:1 layers with ideal composition  $(\text{R}^{2+}, \text{R}^{3+})_3(\text{Si}_{4-x}\text{Al}_x)\text{O}_{10}(\text{OH})_2$  alternating with positively charged brucite-type octahedral interlayer sheets with ideal composition  $(\text{R}^{2+}, \text{R}^{3+})_3(\text{OH})_6$  (Bailey 1988). Electrostatic interactions and a system of hydrogen bonding between the T-O-T layer and the brucite-like sheet contribute to the stability of the structure. Different ways of positioning the T-O-T layer on the interlayer sheet create a large number of regular-stacking polytypes (Bailey 1988). The triclinic *I1b-4* polytype, with symmetry *C1*, and the monoclinic *I1b-2* polytype, with symmetry *C2/m*, are the most abundant regular-stacking one-layer chlorites occurring in nature. The monoclinic structure was described by Zheng and Bailey (1989), Rule and Bailey (1987), and Joswig and Fuess (1989).

Chlorite is among the hydrous phases that may play an important role in upper mantle mass transport and melting processes. In view of its role as a water carrier in subducting slabs, knowledge of the stability field of this hydrous phase may be

obtained by studying its compressibility and the dependence of its crystal structure on pressure.

No high-pressure, single-crystal study has yet been carried out on monoclinic chlorite, the only determination being that on a triclinic polytype (Zanazzi et al. 2006). The aim of the present work on good-quality single-crystal samples is: (1) to investigate the nature of pressure-induced deformation on the atomic arrangement, with particular attention to H-bond system changes in the interlayer region; (2) to compare high-pressure behavior with that of the triclinic polytype coexisting in a rock from Val Malenco (Zanazzi et al. 2006); and (3) to examine how pressure can influence their relative stability, using the opportunity offered by the rock from Val Malenco in which the two polytypes with similar compositions crystallized coevally under the same *P-T* conditions.

### EXPERIMENTAL METHODS

A natural clinochlore from Alpe Raguzzolo, Val Malenco (Eastern Central Alps, Italy), kindly supplied by the Mineralogy Museum, University of Florence (no. 13087/626), was selected for high-pressure X-ray diffraction experiments. According to Müntener et al. (2000), the assemblage olivine + tremolite + chlorite + talc formed in the second stage of the retrograde metamorphism of the Malenco peridotite, during later hydration of ultramafic rocks. Estimated metamorphic conditions were  $0.9 \pm 0.1$  GPa and  $600 \pm 50$  °C. The sample consists of green platy

\* E-mail: zanazzi@unipg.it

crystals of coexisting triclinic and monoclinic chlorite, the latter far less abundant. The chemical composition, as determined on a Cameca SX50 electron microprobe (IGG, Padova section) is nearly the same for the two polytypes. Working conditions were 15 kV and 15 nA with 1  $\mu\text{m}$  beam size, and counting times of 10 s for peak and background. Synthetic pure oxides were used as standards for Mg, Al, Ti, Cr, and Mn, synthetic ferrosilite for Fe, natural wollastonite for Si and Ca, and natural albite for Na. Averaging of three spot analyses yielded the composition (in wt%): NaO 0.01(1), CaO 0.01(1), MgO 31.69(8), TiO<sub>2</sub> 0.03(3), Cr<sub>2</sub>O<sub>3</sub> 0.03(3), MnO 0.08(3), FeO 6.38(27), Al<sub>2</sub>O<sub>3</sub> 14.94(52), SiO<sub>2</sub> 32.44(68), total 85.61. The calculated formula: (Mg<sub>0.09</sub>Fe<sub>0.01</sub>Mn<sub>0.02</sub>Ti<sub>0.01</sub>Cr<sub>0.02</sub>Al<sub>1.80</sub>)<sub>Σ=11.92</sub>(Si<sub>6.33</sub>Al<sub>1.65</sub>)<sub>Σ=8</sub>O<sub>20</sub>(OH)<sub>16</sub>, is in very good agreement with the composition of the triclinic polytype (Zanazzi et al. 2006) and those given in Table 5 of Müntener et al. (2000). The sample is a clinochlore according to the Bayliss (1975) nomenclature.

### Structural refinement at ambient pressure

A crystal of the monoclinic polytype (space group *C2/m*; *I1b-2* polytype; 0.10 × 0.07 × 0.01 mm in size) was mounted on an XCALIBUR (Oxford Diffraction) diffractometer equipped with both CCD area and point detectors, operating at 50 kV and 40 mA, with graphite monochromated MoK $\alpha$  radiation ( $\lambda = 0.7107 \text{ \AA}$ ). Diffraction data were first collected at room conditions with the area detector from the crystal in air. To maximize reciprocal space coverage, a combination of  $\omega$  and  $\phi$  scans was used, with a step size of 0.8° and a time of 32 s/frame, for a total of 711 frames. Data were corrected for absorption with the SADABS program (Sheldrick 1996). Details of data collection and refinement are listed in Table 1. Unit-cell parameters were accurately measured by the point detector and calculated by the least-squares fit of Bragg angles for about 50 selected reflections. The values of symmetry-constrained unit-cell parameters are listed in Table 2. Calculated density, assuming  $Z = 1$ , is  $d_{\text{calc}} = 2.69 \text{ g/cm}^3$ . Crystal structure refinement was carried out with anisotropic displacement parameters by the SHELX-97 program (Sheldrick 1997), starting from the atomic coordinates of Joswig and Fuess (1989). Neutral atomic scattering factors and  $\Delta f'$ ,  $\Delta f''$  coefficients from the *International Tables for Crystallography* (Wilson and Prince 1999) were used. Full occupancy was assumed for all cation sites. The electronic density in the octahedral cation sites was accounted for by fitting the scattering factor curves of Mg and Fe with variable occupancy and that of tetrahedral sites with the curves of Si and Al. The resulting sum of electrons in the cell was 155.9 and 109.0  $e^-$  for octahedral and tetrahedral sites, in good agreement with data calculated on the basis of chemical analysis (159.3 and 110.3  $e^-$ , respectively). The hydrogen atoms were located in the difference electronic density map and included in the last cycles of refinement, with equal isotropic atomic displacement factors and the bond distance from the oxygen constrained to 0.85 ± 0.05  $\text{\AA}$ . At the end of the refinement, no peak larger than 1.1  $e^-/\text{\AA}^3$  was present in the final difference Fourier synthesis. Table 3<sup>1</sup> lists the observed and calculated structure factors. Atomic coordinates are listed in Table 4.

### High-pressure experiments

For high-pressure crystal structure refinements, a chlorite sample with a chip of Sm<sup>2+</sup>:BaFCl and a fragment of  $\alpha$ -quartz were mounted in a Merrill-Bassett diamond anvil cell (DAC), equipped with type-I diamonds with 800  $\mu\text{m}$  culet

face diameter. The pressure chamber was a 380  $\mu\text{m}$  diameter hole, made by spark erosion on a 250  $\mu\text{m}$  thick steel Inconel 750X gasket, preindented to 180  $\mu\text{m}$ . A methanol-ethanol mixture (4:1) was used as hydrostatic pressure-transmitting medium. The wavelength shift of the 6876  $\text{\AA}$  Sm<sup>2+</sup> fluorescence line was measured, for an approximate pressure estimate (Comodi and Zanazzi 1993); the quartz crystal was used for precise measurement of pressure (Angel et al. 1997). Uncertainties in pressure calibration based on the equation of state of quartz were estimated to be less than 0.05 GPa. Experiments were carried out in the pressure range 10<sup>-4</sup>–5.5 GPa. Higher pressure was prevented by failure of the gasket.

The DAC was centered on the diffractometer following the procedure of Budzianowski and Katrusiak (2004). Intensity data were collected with the CCD detector operating in the “fixed- $\phi$ ” mode (Finger and King 1978), corrected for absorption using Absorb V6.0 software (Angel 2004) and then averaged. After each data collection, the unit-cell parameters of chlorite and quartz were accurately measured with the point detector.

Least-squares refinements with data measured at 0.77, 1.52, 2.28, 3.66, 4.52, and 5.47 GPa were performed with the SHELX-97 program (Sheldrick 1997). Isotropic atomic displacement parameters were used for all atoms, and site occupancies were fixed to the values resulting from refinement at ambient pressure. Details of data collections and refinements are listed in Table 1, observed and calculated structure factors in Table 3<sup>1</sup> and fractional atomic coordinates and displacement parameters in Table 4. Table 5 lists bond distances and geometrical parameters at both ambient and higher pressures.

## RESULTS

### Results of refinement at ambient pressure

The structural results of the refinement are in very good agreement with literature data. In particular, partial ordering of trivalent cations in the brucite-type sheet, with preference for the M4 site, as suggested by Joswig and Fuess (1989), is confirmed. Ordering of trivalent cations at M4 is more evident than in the triclinic polytype (Zanazzi et al. 2006), in contrast with the findings of Zheng and Bailey (1989) in intergrown monoclinic and triclinic samples from Kenya. They found that the dominant triclinic polytype was more ordered, and ascribed its greater stability to this structural factor. The tetrahedral T-O mean bond length is 1.652  $\text{\AA}$ , in good agreement with <sup>14</sup>Al content. Tetrahedral rotation angle  $\alpha$  is 6.2°; this angle is the difference between 120° and the  $\Phi$  angles formed by the basal O-O edges of adjacent tetrahedra [ $2\alpha = \sum_{i=1,6} (|120 - \Phi_i|)/6$ , Weiss et al. 1992]. The OH groups of the brucite-type sheet are involved as donors in H-bonds with the basal oxygen atoms of the tetrahedral sheet. The O-O distances are 2.897 and 2.919  $\text{\AA}$ , respectively for the OH2-O2 and OH3-O3 interactions.

### Compressibility

Unit-cell parameters at various pressures are listed in Table 2 and shown in Figure 1. A third-order Birch-Murnaghan Equation of State (EoS) is the best approximation to describe the evolution of chlorite unit-cell volume with  $P$ , as suggested by plotting “normalized stress” vs. Eulerian finite strain (Angel 2000, 2001) (Fig. 2). The resulting EoS parameters are  $V_0 = 703.2(8) \text{ \AA}^3$ , very close

<sup>1</sup> Deposit item AM-07-011, Table 3 (observed and calculated structure factors). Deposit items are available two ways: For a paper copy contact the Business Office of the Mineralogical Society of America (see inside front cover of recent issue) for price information. For an electronic copy visit the MSA web site at <http://www.minsocam.org>, go to the American Mineralogist Contents, find the table of contents for the specific volume/issue wanted, and then click on the deposit link there.

TABLE 1. Details of data collection and refinement at different pressures

$P$ (GPa)	0.0001	0.77	1.52	2.28	3.66	4.52	5.47
$\theta$ -range	3–33°	3–30°	3–30°	3–30°	3–30°	3–30°	3–30°
crystal-detector distance (mm)	65	65	65	65	65	65	65
No. measured reflections	7661	2016	1974	1940	1964	3703	1301
No. independent reflections	1334	303	295	297	296	320	261
Reflections with $I > 4\sigma(I)$	1180	210	190	217	225	235	178
No. refined parameters	92	33	33	33	33	33	33
$R_{\text{int}}$ %	4.4	9.2	10.8	8.5	8.2	9.3	13.7
$R_1$ %	3.6	7.5	6.9	6.5	6.3	7.5	9.6

to the measured value (Table 2),  $K_0 = 71(9)$  GPa, and  $K' = 8(5)$ . Weighted  $\chi^2$  is 4, maximum  $\Delta P$  is 0.3 GPa. The bulk modulus value obtained by fitting data with a second-order EoS ( $K'$  fixed to 4) is 79(3) GPa. These values are lower than those found for the triclinic polytype [ $K_0 = 88(5)$  GPa and  $K' = 5(3)$ , Zanazzi et al. 2006], showing that the symmetry of various polytypes may influence the compression behavior of chlorite.

Literature compressibility data for clinocllore are mostly in reasonable agreement. The bulk moduli determined on both natural and synthetic samples are: 75.4(2.7) GPa (synthetic clinocllore, neutron powder diffraction; Welch and Marshall 2001); 77.6(1.1) GPa (synthetic clinocllore; Grevel et al. 1997); 78.6(1.2) (natural clinocllore; Theye et al. 2003); 81.0(5) GPa (synthetic clinocllore,

synchrotron powder diffraction data; Welch and Crichton 2002); and 89.5(27) GPa (synthetic clinocllore, EDS synchrotron data; Pawley et al. 2002). All these values were obtained at fixed  $K' = 4$  and assuming monoclinic symmetry, or sometimes hexagonal symmetry (Theye et al. 2003). The data of Welch and Marshall (2001) and Grevel et al. (1997) are closest to that of the present study. The main differences between our data and those in the literature probably arise from the different experimental methods employed, single-crystal vs. powder diffraction, and the nature, composition and actual symmetry of the samples. Moreover, the bulk modulus of 47.2 GPa given in the databases of Berman (1988) and Holland and Powell (1998) fits none of the measured values, and consequently needs to be updated.

Both the triclinic and monoclinic *I1b* polytypes of chlorite are more rigid than other layer structures. Their bulk moduli are higher than those of phyllosilicates such as talc (41.6 GPa, Pawley et al. 1995) and micas [54 GPa in phlogopite, Comodi et al. 2004; in the range 52–61 GPa in 2M<sub>1</sub> muscovites, 58–62 GPa in 2M<sub>1</sub> and 3T phengites, 66 GPa in paragonite, see Table 1 in Zanazzi and Pavese (2002) and references therein] or that of brucite (47 GPa, Parise et al. 1994; 41 GPa, Catti et al. 1995;

**TABLE 2.** Unit-cell parameters at different pressures

P (GPa)	a (Å)	b (Å)	c (Å)	$\beta$ (°)	V (Å <sup>3</sup> )
1E-4	5.3363(9)	9.240(1)	14.37(3)	96.93(5)	703.4(4)
0.77	5.327(4)	9.227(5)	14.23(9)	96.9(3)	694(1)
1.52	5.304(3)	9.190(5)	14.20(7)	96.9(2)	687(1)
2.28	5.293(2)	9.168(3)	14.19(3)	96.79(7)	683.8(5)
3.66	5.270(2)	9.132(3)	14.11(4)	96.77(8)	674.3(6)
4.52	5.252(2)	9.103(3)	14.08(3)	96.71(8)	668.4(5)
5.47	5.237(2)	9.078(3)	14.00(3)	96.64(8)	661.1(5)

**TABLE 4.** Fractional atomic coordinates and isotropic displacement parameters  $U_{eq}/U_{iso}$  (Å<sup>2</sup>) at different pressures

Site	x/a	y/b	z/c	$U_{eq}/U_{iso}$	Site	x/a	y/b	z/c	$U_{eq}/U_{iso}$			
T	0.22844(9)	0.16673(5)	0.19152(4)	0.0074(1)	O2	0.2100(4)	0	0.2328(1)	0.0163(4)			
	0.2297(5)	0.1667(2)	0.1933(8)	0.010(1)		0.209(1)	0	0.233(1)	0.014(2)			
	0.2286(7)	0.1664(3)	0.1909(9)	0.005(1)		0.207(2)	0	0.234(2)	0.020(4)			
	0.2284(6)	0.1665(3)	0.1907(8)	0.007(1)		0.204(2)	0	0.233(2)	0.014(3)			
	0.2285(6)	0.1663(3)	0.1921(7)	0.007(1)		0.199(2)	0	0.233(2)	0.011(2)			
	0.2278(6)	0.1666(3)	0.1913(8)	0.007(1)		0.196(2)	0	0.231(2)	0.014(3)			
	0.229(1)	0.1670(6)	0.190(1)	0.004(2)		0.198(4)	0	0.237(3)	0.014(6)			
M1	0	0	0	0.0073(3)	O3	0.5070(3)	0.2344(2)	0.2327(1)	0.0161(3)			
	0	0	0	0.006(1)		0.5077(8)	0.2339(6)	0.234(1)	0.015(2)			
	0	0	0	0.008(2)		0.509(1)	0.2327(8)	0.233(1)	0.017(2)			
	0	0	0	0.006(1)		0.511(1)	0.2321(8)	0.235(1)	0.015(2)			
	0	0	0	0.005(1)		0.514(1)	0.2290(8)	0.237(1)	0.019(2)			
	0	0	0	0.006(2)		0.514(1)	0.2283(9)	0.236(1)	0.018(2)			
	0	0	0	0.008(3)		0.514(3)	0.225(2)	0.235(3)	0.020(5)			
M2	0	0.33269(8)	0	0.0074(2)	OH1	0.1901(3)	½	0.0734(1)	0.0099(3)			
	0	0.3326(3)	0	0.007(1)		0.192(2)	½	0.072(2)	0.011(2)			
	0	0.3328(4)	0	0.007(2)		0.189(2)	½	0.072(2)	0.008(3)			
	0	0.3333(4)	0	0.005(1)		0.188(2)	½	0.073(2)	0.009(3)			
	0	0.3335(4)	0	0.006(1)		0.190(2)	½	0.075(2)	0.008(2)			
	0	0.3334(5)	0	0.006(1)		0.189(2)	½	0.075(2)	0.010(3)			
	0	0.3336(9)	0	0.008(2)		0.192(3)	½	0.077(3)	0.008(5)			
M3	0	0.16654(8)	½	0.0076(2)	OH2	0.1517(4)	0	0.4307(1)	0.0151(4)			
	0	0.1674(3)	½	0.006(1)		0.152(2)	0	0.425(2)	0.013(2)			
	0	0.1677(5)	½	0.004(2)		0.151(2)	0	0.425(2)	0.012(3)			
	0	0.1669(4)	½	0.005(1)		0.150(2)	0	0.425(2)	0.013(3)			
	0	0.1667(4)	½	0.005(1)		0.150(2)	0	0.425(2)	0.010(3)			
	0	0.1672(5)	½	0.005(1)		0.149(2)	0	0.423(2)	0.013(3)			
	0	0.1659(9)	½	0.004(2)		0.150(4)	0	0.423(4)	0.022(6)			
M4	0	½	½	0.0064(3)	OH3	0.1407(3)	0.3368(2)	0.4304(1)	0.0160(3)			
	0	½	½	0.006(1)		0.141(1)	0.3368(5)	0.427(2)	0.015(2)			
	0	½	½	0.005(2)		0.141(2)	0.3364(7)	0.425(2)	0.013(3)			
	0	½	½	0.005(1)		0.142(1)	0.3358(7)	0.426(1)	0.014(2)			
	0	½	½	0.005(1)		0.142(1)	0.3364(7)	0.425(1)	0.013(2)			
	0	½	½	0.005(2)		0.142(2)	0.3361(7)	0.426(1)	0.012(2)			
	0	½	½	0.007(3)		0.140(3)	0.338(1)	0.421(2)	0.014(4)			
O1	0.1914(2)	0.1666(1)	0.07678(9)	0.0087(2)	H1	0.215(9)	½	0.134(3)	0.050(8)			
	0.192(1)	0.1668(5)	0.078(2)	0.006(2)		H2	0.180(10)	0	0.378(3)	0.050(8)		
	0.190(2)	0.1671(7)	0.072(2)	0.011(3)			H3	0.141(8)	0.329(4)	0.378(2)	0.050(8)	
	0.191(1)	0.1671(7)	0.075(2)	0.009(2)								
	0.192(1)	0.1672(6)	0.076(2)	0.008(2)								
	0.192(1)	0.1675(7)	0.074(2)	0.008(2)								
	0.186(2)	0.167(1)	0.071(3)	0.007(3)								

Notes: For each atom values from top to bottom correspond to the refinements at 0.0001, 0.77, 1.52, 2.28, 3.66, 4.52, and 5.47 GPa. The H positions are those from the refinement in air. The occupancy of Mg against Fe in M sites in air refined to 0.912(2), 0.915(2), 0.944(2), and 0.944(2) Mg atoms for M1, M2, M3, and M4 respectively. The occupancy of Si against Al in T site refined to 0.624(4). This value was fixed in the refinements at high pressure. Estimated standard deviations refer to the last digit.

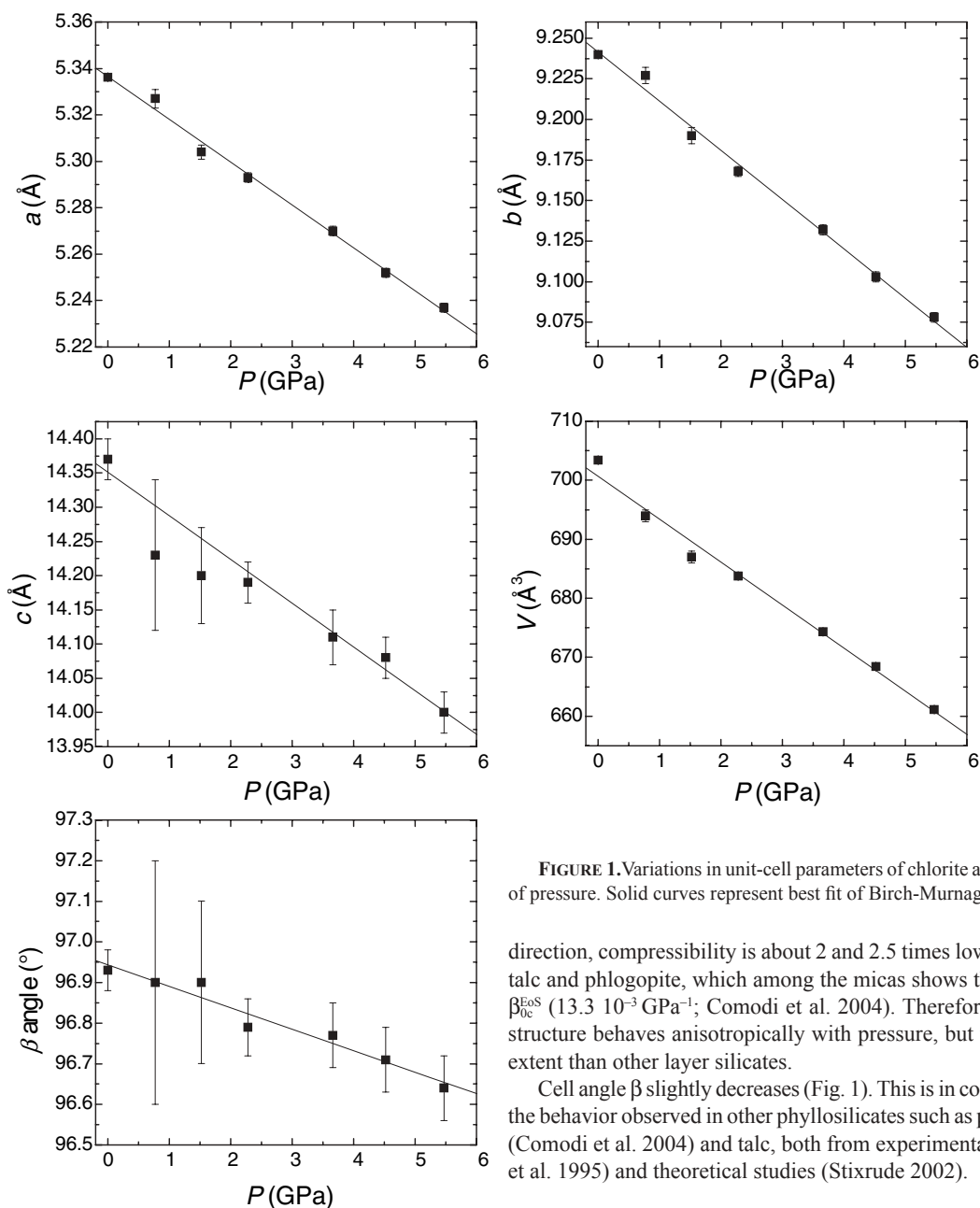


FIGURE 1. Variations in unit-cell parameters of chlorite as a function of pressure. Solid curves represent best fit of Birch-Murnaghan EoS.

direction, compressibility is about 2 and 2.5 times lower than in talc and phlogopite, which among the micas shows the highest  $\beta_{bc}^{EoS}$  ( $13.3 \cdot 10^{-3} \text{ GPa}^{-1}$ ; Comodi et al. 2004). Therefore, chlorite structure behaves anisotropically with pressure, but to a lesser extent than other layer silicates.

Cell angle  $\beta$  slightly decreases (Fig. 1). This is in contrast with the behavior observed in other phyllosilicates such as phlogopite (Comodi et al. 2004) and talc, both from experimental (Pawley et al. 1995) and theoretical studies (Stixrude 2002).

#### Structural evolution with $P$

The stacking sequence of chlorite is characterized by 2:1 talc- and brucite-type sheets, each contributing in a different way to the overall structural response to pressure. We can analyze how each polyhedron in different sheets of chlorite changes with increasing pressure. The volume of the octahedra of the talc-type layer decreases and the octahedral thickness shortens, whereas the octahedra of brucite-type sheets tilt and become more regular with pressure, as shown by the angle variance values (Robinson et al. 1971) and  $\psi$  angles (angle between the body diagonal of the octahedron and the vertical; Bailey 1988) (Table 5). This regularization leads to an increase in volume of the octahedra. As a consequence, thickening along  $c^*$  and a reduction in the  $a$ - $b$  plane of the interlayer octahedral sheet occur; the same

44 GPa, Nagai et al. 2000).

The behavior of clinocllore at high  $P$  is not dissimilar from that of other phyllosilicates and micas. The “axial moduli” obtained by fitting a second-order Birch-Murnaghan EoS to  $a$ ,  $b$ , and  $c$  axes are:  $a_0 = 5.337(1) \text{ \AA}$ ,  $K_0 = 87(2) \text{ GPa}$ ;  $b_0 = 9.241(2) \text{ \AA}$ ,  $K_0 = 92(2) \text{ GPa}$ ; and  $c_0 = 14.36(3) \text{ \AA}$ ,  $K_0 = 62(8) \text{ GPa}$ . Axial compressibility values, obtained by dividing the inverse of the axial moduli by three, are:  $\beta_{0a}^{EoS} = 3.8(1)$ ,  $\beta_{0b}^{EoS} = 3.6(1)$ , and  $\beta_{0c}^{EoS} = 5.4(5) \cdot 10^{-3} \text{ GPa}^{-1}$ . Clinocllore has greater compressibility in the  $ab$  plane compared to other layer silicates, e.g., phlogopite, for which axial compressibilities along  $a$  and  $b$  axes are 2.7 and  $2.6 \cdot 10^{-3} \text{ GPa}^{-1}$ . Axis  $c$  is the most affected by pressure due to the layered nature of the phase; nevertheless, along the [001]

**TABLE 5.** Values of bond distances (Å), polyhedral volumes (Å<sup>3</sup>), and distortion parameters (following Robinson et al. 1971) at different pressures

<i>P</i> (GPa)	0.0001	0.77	1.52	2.28	3.66	4.52	5.47
T-O1	1.637(1)	1.63(2)	1.67(3)	1.64(2)	1.62(2)	1.64(2)	1.66(3)
T-O2	1.6581(9)	1.650(8)	1.66(1)	1.65(1)	1.64(1)	1.63(1)	1.67(2)
T-O3	1.655(1)	1.646(7)	1.65(1)	1.67(1)	1.66(1)	1.66(1)	1.64(2)
T-O3	1.658(2)	1.655(6)	1.66(1)	1.66(1)	1.66(1)	1.65(1)	1.67(2)
<T-O>	1.652	1.65	1.66	1.65	1.65	1.65	1.66
<i>V</i> <sub>T</sub>	2.31	2.29	2.34	2.31	2.28	2.28	2.33
σ <sup>2</sup> T*	2.332	1.10	4.23	6.87	6.19	5.54	12.08
λ <sub>T1</sub> †	1.001	1.000	1.001	1.002	1.001	1.001	1.003
Tetr. rot. α‡	6.2	6.3	6.9	7.2	8.3	8.6	9.3
T sheet thickness	2.225	2.21	2.27	2.25	2.23	2.24	2.29
M1-O1 ×4	2.088(1)	2.09(1)	2.04(2)	2.06(1)	2.06(1)	2.04(1)	2.00(2)
M1-OH1 ×2	2.066(2)	2.04(1)	2.04(2)	2.05(1)	2.05(1)	2.04(2)	2.04(3)
<M1-O>	2.081	2.07	2.04	2.06	2.06	2.04	2.02
<i>V</i> <sub>M1</sub>	11.83	11.7	11.1	11.3	11.5	11.2	10.7
Ψ <sub>M1</sub> §	58.8	58.8	60.1	59.5	58.9	59.4	59.7
σ <sup>2</sup> <sub>M1</sub> *	33.53	35.34	58.75	46.04	35.70	45.03	52.00
λ <sub>M1</sub> †	1.010	1.011	1.018	1.014	1.011	1.014	1.016
M2-O1 ×2	2.084(1)	2.08(1)	2.04(2)	2.05(2)	2.06(1)	2.03(1)	2.00(2)
M2-O1 ×2	2.090(1)	2.09(1)	2.04(2)	2.05(1)	2.05(1)	2.03(1)	2.02(2)
M2-OH1 ×2	2.067(1)	2.06(1)	2.04(2)	2.04(2)	2.05(2)	2.04(2)	2.05(3)
<M2-O>	2.080	2.08	2.04	2.05	2.05	2.03	2.02
<i>V</i> <sub>M2</sub>	11.82	11.7	11.0	11.2	11.3	11.0	10.8
Ψ <sub>M2</sub> §	58.8	58.9	60.0	59.4	58.8	59.2	59.9
σ <sup>2</sup> <sub>M2</sub> *	33.68	36.02	56.96	43.71	33.42	41.61	54.28
λ <sub>M2</sub> †	1.010	1.011	1.018	1.013	1.010	1.013	1.017
O sheet thickness#	2.158	2.15	2.04	2.09	2.13	2.08	2.03
M3-OH2 ×2	2.052	2.09(1)	2.09(2)	2.07(1)	2.06(1)	2.07(1)	2.06(3)
M3-OH3 ×2	2.053(2)	2.06(1)	2.07(2)	2.06(1)	2.05(1)	2.05(1)	2.09(2)
M3-OH3 ×2	2.055(2)	2.07(1)	2.07(2)	2.06(1)	2.07(1)	2.04(1)	2.08(2)
<M3-O>	2.053	2.08	2.07	2.06	2.06	2.05	2.07
<i>V</i> <sub>M3</sub>	11.10	11.6	11.6	11.5	11.4	11.3	11.8
Ψ <sub>M3</sub> §	61.1	59.9	59.5	59.5	59.3	59.3	58.3
σ <sup>2</sup> <sub>M3</sub> *	81.97	54.35	46.57	47.60	42.87	42.52	28.19
λ <sub>M3</sub> †	1.026	1.017	1.014	1.015	1.013	1.013	1.008
M4-OH2 ×2	2.000(2)	2.03(2)	2.02(2)	2.02(2)	2.02(2)	2.02(2)	2.01(3)
M4-OH3 ×4	2.006(2)	2.03(1)	2.03(2)	2.03(1)	2.03(1)	2.02(1)	2.03(2)
<M4-O>	2.004	2.03	2.03	2.03	2.02	2.02	2.03
<i>V</i> <sub>M4</sub>	10.41	10.9	11.0	10.9	10.9	10.8	11.0
Ψ <sub>M4</sub> §	60.3	59.0	58.7	58.9	58.6	58.7	57.5
σ <sup>2</sup> <sub>M4</sub> *	63.09	38.10	32.82	36.34	31.79	31.60	16.34
λ <sub>M4</sub> †	1.020	1.012	1.010	1.011	1.010	1.010	1.004
O sheet thickness	1.984	2.09	2.11	2.09	2.11	2.10	2.18
T-O-T···O distance**	2.821	2.72	2.70	2.70	2.65	2.66	2.59
T-O-T thickness	6.608	6.56	6.58	6.59	6.59	6.56	6.61
OH2-O2	2.897(3)	2.78(3)	2.76(4)	2.78(3)	2.75(3)	2.75(4)	2.65(7)
OH3-O3	2.919(2)	2.83(2)	2.81(3)	2.79(3)	2.73(2)	2.74(3)	2.67(5)

Notes: Estimated standard deviations refer to the last digit.

\* σ<sup>2</sup> is the angle variance (deg<sup>2</sup>).

† λ is the quadratic elongation.

‡ α is the tetrahedral rotation angle (deg); see text for definition.

§ Ψ is the octahedral flattening angle (deg); see text for definition.

# Thickness of the octahedral sheet of the talc-like layer.

|| Mean thickness of the brucite-like layer.

\*\* Mean distance between talc-like layer and brucite-type sheet.

mechanism is observed in brucite (Parise et al. 1994; Nagai et al. 2000) and triclinic polytype (Zanazzi et al. 2006). In contrast, tetrahedral distortion increases with *P*, whereas tetrahedral thickness and volume remain almost unchanged (Table 5). Tetrahedral distortion at high pressure may also be ascribed to the increased hydrogen bond strength between the OH of the brucite-type sheet and the basal O of the tetrahedral sheet.

As in all layer silicates, an increase in the ditrigonalization of the sixfold tetrahedral rings is required to facilitate size matching between the relatively incompressible tetrahedral and the more compressible octahedral sheets. Increasing ditrigonalization is shown by the increase in tetrahedral rotation angle α from 6.2 to 9.3° with pressure. It results both from the requirement for fitting the octahedral and tetrahedral sheets and from the strengthening of OH-O hydrogen bonds due to thinning of the space between

talc-like layer and brucite-like sheet and consequent shortening of O-O distance with *P*.

In the pressure range studied here, the thickness of the brucite-type sheet increases by about 10%, whereas that of T-O-T layer does not change: on the contrary, the distance between T-O-T layer and brucite-type sheet, i.e., the thickness of the region in which H-bonds are located, is reduced by about 8%. Despite the increased thickness of the brucite-type sheet, the greatest contraction of the structure occurs along the [001] direction. Around 5 GPa, the OH-O distance approaches 2.7 Å, the limit below which the two O<sup>2-</sup> are considered to be in contact (Brown 1976). At higher pressures, anomalous structural behavior may occur. The spectroscopic study of Kleppe et al. (2003) showed a strong discontinuity with a large increase in *dv/dP* for the OH mode of the brucite-type sheet at 9–10 GPa. The high positive

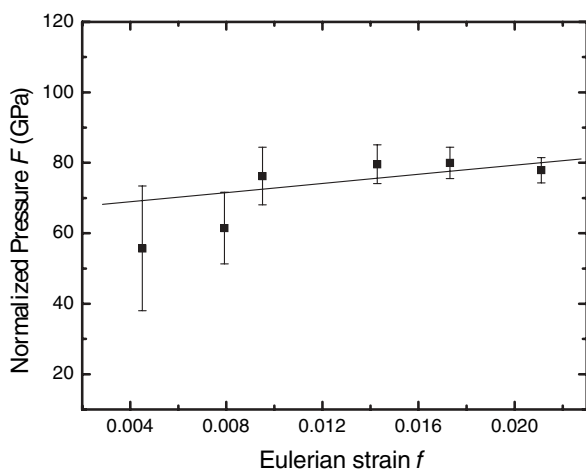


**FIGURE 2.** Plot of “normalized stress” defined as  $F_E = P/[3f_E(1 + 2f_E)^{5/2}]$  vs. finite strain  $f_E = [(V_0/V)^{2/3} - 1]/2$ . The two lower values were omitted from computations. Chlorite unit-cell volume data are adequately described by a third-order truncation of EoS.

shifts of the O-H mode with  $P$  were reported by Hofmeister et al. (1999) to be due to H-H cation repulsion, as a consequence of the decreased OH-O angle. Neutron diffraction data for clinoclchlore show a considerable decrease in the OH-O angle, from 170 to 155° (Welch and Marshall 2001). The in-plane movement of basal oxygen atoms by tetrahedral rotation suggests a decrease in the OH-O angle. The repulsive effects caused by interlayer shortening may explain why compressibility along axis  $c$  is smaller than in other layer silicates, together with the lower anisotropy and the peculiar stiffer character of chlorite.

#### Implications for polytype stability

There are only a few studies on the energetic and thermodynamic stability of various chlorite polytypes and these mainly concern the effect of temperature on chlorite polymorphism from type I to type II structures (Hayes 1970; Walker 1989). On the basis of cation-cation repulsion and cation-anion attraction possible in the various layer sequences, Bailey (1988) estimated that the type IIb layer sequence is the most stable. Zheng and Bailey (1989), studying intergrown type IIb monoclinic and triclinic clinoclchlores from Kenya, found no structural differences, apart from slightly less ordering of trivalent cations in the brucite-type octahedral layer in the monoclinic form compared to our results. Cell volumes, recalculated from the reported unit-cell parameters, are 700.5 and 701.2 Å<sup>3</sup> for triclinic and monoclinic cells, respectively. On the basis of textural relations between the phases, Zheng and Bailey (1989) suggested that the monoclinic IIb-2 structure is less stable than the triclinic IIb-4 form.

In the rock from Val Malenco both triclinic and monoclinic polytypes coexist, with very similar chemical composition and slightly different unit-cell volumes (701.7 and 703.4 Å<sup>3</sup>, respectively). We therefore had the opportunity of comparing the high-pressure behavior of both monoclinic and triclinic forms (Zanazzi et al. 2006), and contributing to knowledge of their relative stability in a natural environment. The bulk modulus value of 71 GPa, measured in this work for monoclinic clinoclchlore is

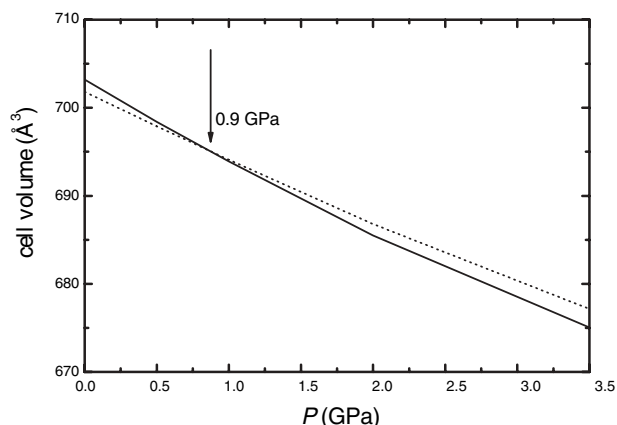


**FIGURE 3.** Isothermal equations of state showing unit-cell volumes of two clinoclchlore polytypes as a function of pressure: monoclinic (solid line) and triclinic (dashed).

less than the 88 GPa found for the triclinic polytype (Zanazzi et al. 2006), although the difference in the relative compressibilities of the two polytypes must be viewed with caution, owing to relative data uncertainty (the differences between  $K_0$  and  $K'$  are of the order of 1–2  $\sigma$ ). The decrease in molar volumes as a function of  $P$  was computed with the isothermal EoS for the two polytypes (Fig. 3). The curves cross at  $P = 0.9$  GPa. Since pressure tends to stabilize the phase with smaller molar volume, the triclinic polytype is favored in low-pressure regimes. Monoclinic clinoclchlore is more compressible than the triclinic type: at high pressure, the  $P$ - $V$  contribution to Gibbs energy tends to favor the former. These considerations, based on small differences only in terms of pure elastic energy, are of course not fully conclusive, since we did not take into account the effect of temperature, and assumed that the thermal expansion coefficients and  $dK/dT$  were equal for both polytypes. Nonetheless, our results support the hypothesis that pressure conditions do play a role in stabilizing the different polytypes of clinoclchlore, explaining the relatively greater abundance of triclinic forms in nature, when the pressure of chlorite crystallization is less than 0.9 GPa. The triclinic form is dominant in our sample from Val Malenco, and in the Kenyan sample described by Zheng and Bailey (1989), in agreement with assumptions regarding the relative stability of the two polytypes, based on the textural evidence recorded in the Kenyan sample.

#### ACKNOWLEDGMENTS

The chlorite specimen was kindly supplied by G. Pratesi, Mineralogy Museum of University of Florence. This research was funded by Italian MURST grants to P.F.Z. (COFIN 2005-2006, “Studio delle variazioni cristallografiche indotte da temperatura e pressione nei minerali”) and P.C. (COFIN 2004-2005, “Vincoli naturali (Ulten Zone, Italia) e sperimentali sul ruolo delle fasi idrate nei processi di interazione crosta-mantello”). The authors thank Associate Editor Edward Grew and two anonymous referees for their helpful comments. The English text was revised by Gabriel Walton.

#### REFERENCES CITED

- Angel, R.J. (2000) Equation of State. In R.M. Hazen and R.T. Downs, Eds., *High-Temperature and High-Pressure Crystal Chemistry*, 41, p. 35–59. Reviews in Mineralogy and Geochemistry, Mineralogical Society of America, Chantilly, Virginia.
- (2001) EOS-FIT V6.0 computer program. Crystallography Laboratory, Department Geological Sciences, Virginia Tech, Blacksburg.
- (2004) Program for absorption. Crystallography Laboratory, Department

- Geological Sciences, Virginia Tech, Blacksburg.
- Angel, R.J., Allan, D.R., Miletich, R., and Finger, L.W. (1997) The use of quartz as an internal pressure standard in high pressure crystallography. *Journal of Applied Crystallography*, 30, 461–466.
- Bailey, S.W. (1988) Chlorites: structures and crystal chemistry. In S.W. Bailey Ed., *Hydrous Phyllosilicates (exclusive of micas)*, 19, p. 347–403. Reviews in Mineralogy and Geochemistry, Mineralogical Society of America, Chantilly, Virginia.
- Bayliss, P. (1975) Nomenclature of the trioctahedral chlorites. *Canadian Mineralogist*, 13, 178–180.
- Berman, R.G. (1988) Internally consistent thermodynamic data for minerals in the system  $\text{Na}_2\text{O}-\text{K}_2\text{O}-\text{CaO}-\text{MgO}-\text{FeO}-\text{Fe}_2\text{O}_3-\text{Al}_2\text{O}_3-\text{SiO}_2-\text{TiO}_2-\text{H}_2\text{O}-\text{CO}_2$ . *Journal of Petrology*, 29, 445–552.
- Brown, I.D. (1976) On the Geometry of O-H...O Hydrogen Bonds. *Acta Crystallographica*, A32, 24–31.
- Budzianowski, A. and Katrusiak, A. (2004) High-pressure crystallographic experiments with a CCD-detector. In A. Katrusiak and P. McMillan, Eds., *High-Pressure Crystallography*, p. 101–112. Kluwer Academic Publishers, The Netherlands.
- Catti, M., Ferraris, G., Hull, S., and Pavese, A. (1995) Static compression and H disorder in brucite,  $\text{Mg}(\text{OH})_2$ , to 11 GPa: a powder neutron diffraction study. *Physics and Chemistry of Minerals*, 22, 200–206.
- Comodi, P. and Zanazzi, P.F. (1993) Improved calibration curve for the  $\text{Sm}^{2+}$ :BaFCl pressure sensor. *Journal of Applied Crystallography*, 26, 843–845.
- Comodi, P., Fumagalli, P., Montagnoli, M., and Zanazzi, P.F. (2004) A single-crystal study on the pressure behavior of phlogopite and petrological implications. *American Mineralogist*, 89, 647–653.
- Finger, L.W. and King, H.E. (1978) A revised method of operation of the single-crystal diamond cell and refinement of the structure of NaCl at 32 kbar. *American Mineralogist*, 63, 337–342.
- Grevel, K., Fasshauer, D.W., and Erzner, S. (1997) New compressibility data for clinocllore, kyanite, Mg-chloritoid and Mg-stauroilite. *European Journal of Mineralogy*, 1, 138.
- Hayes, J.B. (1970) Polytypism of chlorite in sedimentary rocks. *Clays and Clay Minerals*, 18, 285–306.
- Hofmeister, A.M., Cynn, H., Burnley, P.C., and Meade, C. (1999) Vibrational spectra of dense, hydrous magnesium silicates at high pressure: Importance of hydrogen bond angle. *American Mineralogist*, 84, 454–464.
- Holland, T.J.B. and Powell, R. (1998) An internally consistent thermodynamic data set for phases of petrological interest. *Journal of Metamorphic Geology*, 16, 309–343.
- Joswig, W. and Fuess, H. (1989) Neutron diffraction study of a one-layer monoclinic chlorite. *Clays and Clay Minerals*, 37, 511–514.
- Kleppe, A.K., Jephcoat, A.P., and Welch, M.D. (2003) The effect of pressure upon hydrogen bonding in chlorite: a Raman spectroscopic study of clinocllore to 26.5 GPa. *American Mineralogist*, 88, 567–573.
- Müntener, O., Hermann, J., and Trommsdorff, V. (2000) Cooling history and exhumation of lower-crustal granulite and upper mantle (Malenco, Eastern Central Alps). *Journal of Petrology*, 41, 175–200.
- Nagai, T., Hattori, T., and Yamanaka, T. (2000) Compression mechanism of brucite: An investigation by structural refinement under pressure. *American Mineralogist*, 85, 760–764.
- Parise, J.B., Leinenweber, K., Weidner, D.J., Tan, K., and Von Dreele, R.B. (1994) Pressure-induced H bonding: Neutron diffraction study of brucite,  $\text{Mg}(\text{OH})_2$ , to 9.3 GPa. *American Mineralogist*, 79, 193–196.
- Pawley, A.R., Redfern, S.A.T., and Wood, B.J. (1995) Thermal expansivities and compressivities of hydrous phases in the system  $\text{MgO}-\text{SiO}_2-\text{H}_2\text{O}$ : talc, phase A and 10 Å phase. *Contributions to Mineralogy and Petrology*, 122, 301–307.
- Pawley, A.R., Clark, S.M., and Chinnery, N.J. (2002) Equation of state measurements of chlorite, pyrophyllite, and talc. *American Mineralogist*, 87, 1172–1182.
- Robinson, K., Gibbs, G.V., and Ribbe, P.H. (1971) Quadratic elongation, a quantitative measure of distortion in coordination polyhedra. *Science*, 172, 191–193.
- Rule, A.C. and Bailey, S.W. (1987) Refinement of the crystal structure of a monoclinic ferroan clinocllore. *Clays and Clay Minerals*, 35, 129–138.
- Sheldrick, G.M. (1996) SADABS. Program for empirical absorption correction of area detector data. Institut für Anorganische Chemie, University of Göttingen, Germany.
- (1997) SHELX-97. Programs for crystal structure determination and refinement. Institut für Anorganische Chemie, University of Göttingen, Germany.
- Stixrude, L. (2002) Talc under tension and compression: Spinodal instability, elasticity, and structure. *Journal of Geophysical Research*, 107, 2327–2336.
- Theye, T., Parra, T., and Lathe, C. (2003) Room temperature compressibility of clinocllore and chamosite. *European Journal of Mineralogy*, 15, 465–468.
- Walker, J.R. (1989) polytypism of chlorite in very low-grade metamorphic rocks. *American Mineralogist*, 74, 738–743.
- Weiss, Z., Rieder, M., and Chmielová, M. (1992) Deformation of coordination polyhedra and their sheets in phyllosilicates. *European Journal of Mineralogy*, 4, 665–682.
- Welch, M.D. and Crichton, W.A. (2002) Compressibility of clinocllore to 8 GPa at 298 K and a comparison with micas. *European Journal of Mineralogy*, 14, 561–565.
- Welch, M.D. and Marshall, W.G. (2001) High-pressure behavior of clinocllore. *American Mineralogist*, 86, 1380–1386.
- Wilson, A.J.C. and Prince, E., Eds. (1999) *International Tables for X-ray Crystallography, Volume C: Mathematical, physical and chemical tables (2nd ed.)*. Kluwer Academic, Dordrecht.
- Zanazzi, P.F. and Pavese, A. (2002) Behavior of micas at high pressure and high temperature. In A. Mottana, F.P. Sassi, J.B. Thompson, Jr., and S. Guggenheim, Eds., *Micas: Crystal Chemistry and Metamorphic Petrology*, 46, p. 99–116. Reviews in Mineralogy and Geochemistry, Mineralogical Society of America, Chantilly, Virginia.
- Zanazzi, P.F., Montagnoli, M., Nazzareni, S., and Comodi, P. (2006) Structural effects of pressure on triclinic chlorite: A single-crystal study. *American Mineralogist*, 91, 1871–1878.
- Zheng, H. and Bailey, S.W. (1989) Structures of intergrown triclinic and monoclinic *11b* chlorites from Kenya. *Clays and Clay Minerals*, 37, 308–316.

MANUSCRIPT RECEIVED JUNE 7, 2006

MANUSCRIPT ACCEPTED OCTOBER 23, 2006

MANUSCRIPT HANDLED BY EDWARD GREW